Bioorganic & Medicinal Chemistry xxx (2016) xxx–xxx

Contents lists available at ScienceDirect

Bioorganic & Medicinal Chemistry

journal homepage: www.elsevier.com/locate/bmc

Synthesis and biological evaluation of analogues of the potent ADAM8 inhibitor cyclo(RLsKDK) for the treatment of inflammatory diseases and cancer metastasis

Victor Yim [a,†], Anaïs F. M. Noisier [a,†,‡], Kuo-yuan Hung [a], Jörg W. Bartsch [b], Uwe Schlomann [b], Margaret A. Brimble [a,c,*]

[a] School of Biological Sciences and The Maurice Wilkins Centre for Molecular Biodiscovery, The University of Auckland, 3a Symonds St, Auckland Central 1010, New Zealand
[b] Department of Neurosurgery, Marburg University, University Hospital, Baldingerstr., 35053 Marburg, Germany
[c] School of Chemical Sciences, The University of Auckland, 23 Symonds St, Auckland 1010, New Zealand

ARTICLE INFO

Article history:
Received 23 May 2016
Revised 20 June 2016
Accepted 21 June 2016
Available online xxxx

Keywords:
ADAM8 inhibitors
Cancer metastasis
Cyclic peptides
Peptidomimetics
SAR study

ABSTRACT

The metalloproteinase ADAM8 serves as a pivotal catalyst in the development of inflammatory diseases and cancer metastasis. The cyclic peptide cyclo(RLsKDK) has been shown to inhibit the enzymatic activity of ADAM8 with high specificity and potency. Herein we report a structure–activity relationship (SAR) study of cyclo(RLsKDK) that involves the synthesis and biological evaluation of the lead compound and structural analogues thereof. This study provides insight into the ligand–receptor interactions that govern the binding of cyclo(RLsKDK) to the ADAM8 disintegrin domain and represents a stepping stone for the development of new treatments for inflammatory diseases and cancer metastasis.

1. Introduction

A disintegrin and metalloproteinase domain 8 (ADAM8) is a catalytically active member of the ADAMs family of proteins, primarily expressed in several tissues including the brain, bone and spinal cord during embryonic development.[1,2] Under inflammatory conditions ADAM8 is up-regulated in most immune cells of the central nervous system[3] and in the lungs.[4] ADAM8 is also associated with allergic responses[5] and is overexpressed in various cancers including lung, prostate and pancreatic adenocarcinomas, brain tumours, and renal cell carcinoma.[6] Furthermore, the levels of ADAM8 expression are strongly correlated with tumour malignancy and invasive activity.[7]

ADAM8 is a transmembrane protein, which possesses a multidomain architecture (Fig. 1). Its extracellular domain consists of several subdomains, among which the pro-peptide, metalloproteinase and disintegrin subdomains are key to the overall activity of the enzyme.[8] ADAM8 activation is an autocatalytic process which is triggered by either homodimeric binding of another ADAM8 or heterodimeric binding of other cell-adhesion molecules to the disintegrin domain.[9] Such dimerisation induces cleavage of the pro-peptide, which in turn triggers a conformational change of the metalloproteinase subdomain, thus exposing the catalytically active site (Fig. 1). The metalloproteinase subdomain then cleaves the extracellular segments of membrane-bound proteins such as cell adhesion molecules or extracellular matrix proteins through a shedding process.[1] Shedding of transmembrane proteins releases extracellular molecules such as growth factors, hormones and chemokines, which then trigger metabolic signalling pathways that give rise to various physiological effects.[10] Furthermore, protein shedding of its extracellular domain is a prerequisite to a regulated intramembrane proteolysis (RIP) event resulting in the release of intracellular molecules that in turn induce intracellular signalling pathways (Fig. 1).[1]

Owing to the significant role of ADAM8 in the mediation of intra- and extracellular signalling pathways involved in inflammatory conditions and cancer, inhibition of ADAM8 activity poses an attractive strategy for the treatment of these diseases. Unfortunately, previous efforts directed at inhibition of ADAM activity failed to deliver useful therapeutic outcomes due to the lack of specificity for a particular enzyme. Both Marimastat and

* Corresponding author. Tel.: +64 937 375 99; fax: +64 937 374 22.
E-mail address: m.brimble@auckland.ac.nz (M.A. Brimble).

† These authors contributed equally to this work.
‡ Institute for Research in Biomedicine (IRB Barcelona), Baldiri Reixac 10, 08028 Barcelona, Spain.

http://dx.doi.org/10.1016/j.bmc.2016.06.042
0968-0896/

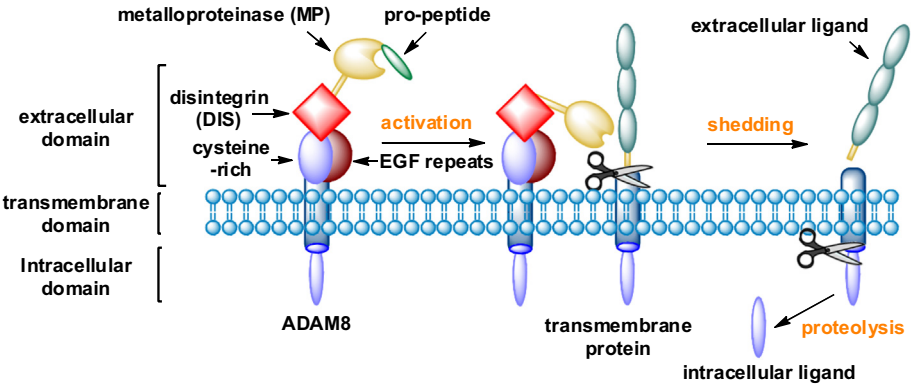

Figure 1. Structure of ADAM8 and its catalytic activity.

Batimastat are examples of broad-spectrum metalloproteinase inhibitors for the treatment of cancer, for which clinical development was terminated due to their deleterious side-effects.[11]

Previous work by Bartsch and Koller[12] focused on a novel approach based on the disruption of multimeric binding to the ADAM8 disintegrin domain, potentially inhibiting ADAM8 proteolytic activity and downstream signalling with unique selectivity. They postulated that peptides mimicking the structure of the integrin binding loop contained in the disintegrin domain would provide potent ADAM8 inhibitors. The binding loop of an ADAM protease is commonly comprised of six amino acids flanked by conserved cysteine residues. Bartsch and Koller designed a short cyclic peptide, cyclo(RLsKDK), based on the sequence of amino acids located within the DIS loop of murine ADAM8 and demonstrated that cyclo(RLsKDK) blocked ADAM8 activation with high potency (IC_{50} = 182 nM) and high specificity, with in vivo efficacy in a pancreatic cancer model (Fig. 2).[13] The serine residue was incorporated as a D-amino acid (where 's' is used to denote D-serine) to favour the formation of a β-turn,[14] thus allowing the presentation of the peptide sequence in a secondary structure closely resembling the integrin-binding loop. The use of D-amino acids also imparts the peptide with greater resistance to proteolytic degradation. Although the discovery of cyclo(RLsKDK) represents a key milestone in the treatment of inflammatory diseases and cancer metastasis, the development of more potent and more stable peptidomimetics is required to identify a valid drug candidate for clinical trials.

In this report, we describe the synthesis and SAR study of a library of peptidomimetics based on the cyclo(RLs^{4}KD^{6}K) lead motif. A systematic substitution approach was used to generate two series of analogues. In the first series, the original D-serine was replaced by L-serine, β-homoserine (hS_β), β-alanine (A_β) and 3-carboxy-β-alanine in order to evaluate the contribution of the hydroxyl group on the peptide activity. Through these substitutions, we expected to probe the effect of modifying the α-chain length, and of altering the spatial conformation of the side-chain. The second series of analogues focused on substitution of arginine (R), leucine (L) and ^{6}lysine (^{6}K) with non-proteinogenic derivatives to determine the impact of these structural substituents on the binding. The aspartic acid (D) residue of cyclo(RLsKDK) was left unmodified as it was previously shown to be crucial for binding.[12]

2. Results and discussion

2.1. Peptide synthesis

All the peptides reported herein were synthesised using the general synthetic pathway described in Scheme 1. First, the linear

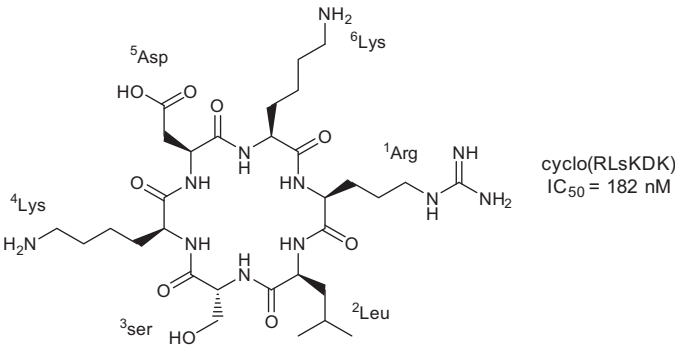

Figure 2. Structure of lead peptide cyclo(RLsKDK).

peptides were assembled by Fmoc solid-phase peptide synthesis (SPPS) using aminomethyl polystyrene (PS) resin derivatised with highly acid-labile 4-(4-hydroxymethyl-3-methoxyphenoxy)-butyric acid (HMPB) linker.[15] HMPB was chosen as only mild conditions are required to effect peptide release from the resin, therefore affording the side-chain protected peptides, necessary for in-solution cyclisation. When applicable, the β-amino acids were chosen as the optimal point for cyclisation, thus avoiding troublesome epimerisation during the head-to-tail macro-cyclisation step.

The desired C-terminal amino acid residues were attached to the resin via an ester bond. The β-alanine, which served as a readily available surrogate for the more expensive hS_β, was used to establish a robust esterification protocol. Thus, Fmoc-β-alanine was esterified with the linker-modified resin using DIC and 1 equiv of DMAP under microwave irradiation (25 W, 50 °C), giving an acceptable loading of 0.46 mmol/g (60% yield) as determined by UV spectrophotometry.[16] Fmoc-hS_β(^{t}Bu)-OH was also successfully coupled to the resin using these conditions (0.38 mmol/g, 52% yield). The peptide containing the 3-carboxy-β-alanine residue was prepared using the same esterification protocol where Fmoc-Asp-OAll (All = allyl) was attached to the resin through its unprotected β-carboxylic acid. For esterification of Fmoc-L-Ser(^{t}Bu)-OH or Fmoc-D-Ser(^{t}Bu)-OH only 0.1 equiv of DMAP was employed to prevent racemisation at the α-carbon. The peptide was then elongated in an automated peptide synthesiser using HCTU as the coupling reagent. When non-proteinogenic amino acids were incorporated, the more potent HATU was used in conjunction with microwave irradiation (25 W, 50 °C) to ensure complete acylation. After assembly of the peptide sequence and removal of the N-terminal Fmoc protecting group, the linear peptides were cleaved from the resin with a solution of TFA in CH_2Cl_2 (5/95 v/v) without loss of side-chain protecting groups. The peptides were then

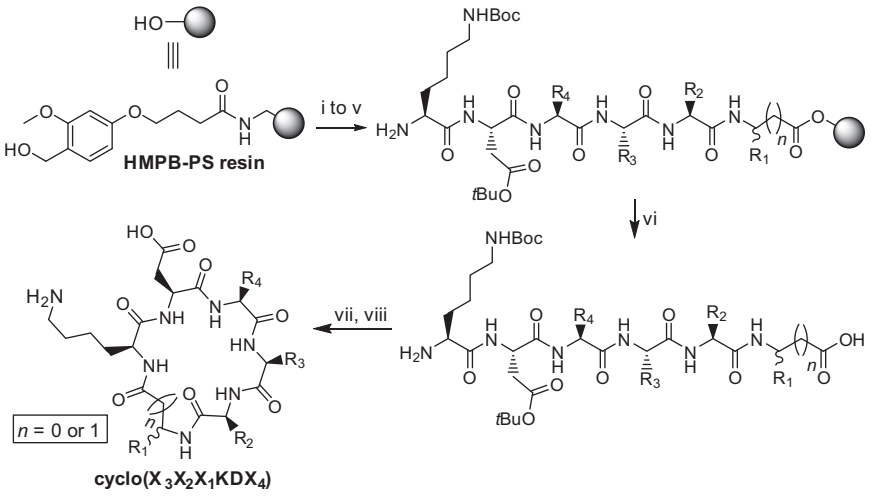

Scheme 1. General synthetic pathway. *Reagents and conditions:* (i) Fmoc-AA-OH or Fmoc-Asp-OAll, DIC, DMAP, DMF/CH_2Cl_2 (20/80 v/v), microwave (25 W, 50 °C), 1 h; (ii) piperidine/DMF (20/80 v/v), 2 × 5 min, rt; (iii) Fmoc-AA-OH, HCTU, NMM, DMF, 45 min, rt or Fmoc-AA-OH, HATU, $^{i}Pr_2NEt$, DMF, microwave (25 W, 50 °C), 1 h; (iv) repeat (ii) and (iii); (v) piperidine/DMF (20/80 v/v), 2 × 5 min, rt; (vi) TFA/CH_2Cl_2 (99.5/0.5 v/v), 8 × 5 min; (vii) HBTU, $^{i}Pr_2NEt$, CH_2Cl_2/DMF, 5 days or HBTU, HOBt, $^{i}Pr_2NEt$, CH_2Cl_2/DMF, 5 days; (viii) TFA/$^{i}Pr_3SiH/H_2O$, 2 h, rt (AA = amino acid).

subjected to macrocyclisation at high dilution to avoid formation of linear or cyclic oligomers.[17] Two different conditions were employed for this key cyclisation step: for peptides containing hS_β, β-alanine, or Asp-OAll at the C-terminus, the reaction was carried out with HBTU/$^{i}Pr_2NEt$ in a solution of DMF in CH_2Cl_2 (10/90 v/v) at a final peptide concentration of 0.9 mg/mL; for peptides containing either L-serine or D-serine at the C-terminus, HOBt was included in the reaction mixture to minimise racemisation. Finally, the side-chain protecting groups were removed with a cocktail solution of TFA/iPr_3SiH/H_2O (95/2.5/2.5 v/v), to afford the crude cyclic products that were purified by RP-HPLC. For peptide **5** (Table 1), the allyl protecting group of the aspartic acid residue was removed with $Pd(PPh_3)_4$ prior to orthogonal side-chain deprotection. A focused library of nineteen peptides (Table 1) was prepared following this synthetic procedure.

2.2. Biological evaluation

The inhibitory activity of all synthetic peptides against the release of CD23 antibody mediated by ADAM8 was measured using an enzyme-linked immunosorbent assay (ELISA). The IC_{50} values obtained for each peptide are reported in Table 1.

We began our SAR study by investigating the effect of modifying the non-proteinogenic D-serine residue within the cyclo (RLsKDK) peptide sequence. Peptide **2** where the D-amino acid was replaced by its L-enantiomer showed a slight decrease in potency. Little improvement was achieved by switching from D-serine to β-homoserine. Interestingly, both the complete removal of the hydroxyl group as in peptide **4**, or its substitution by a carboxylic acid moiety as in peptide **5** showed a detrimental effect on activity. A respective 2.5 and 10-fold increase in IC_{50} was observed for peptides **5** and **4** with respect to **3**. The significant effect of the hydroxyl group on peptide inhibitory activity could be attributed to the existence of polar interactions between the ligand hydroxyl side-chain and the receptor binding-surface.

Despite the decreased potency of peptide **4**, β-alanine was employed as a readily available surrogate of β-homoserine within our second series of peptidomimetics. The focus of the study shifted to investigating the activity of derivatives of **4** where arginine, leucine and ^{6}lysine were consecutively substituted with non-proteinogenic analogues (see Series 2 in Table 1). Replacement of arginine with nitroarginine (peptide **6**) had a detrimental effect

Table 1
The IC_{50} values of synthetic peptides **1**–**19**

No.	Peptides	IC_{50} (nM)
Series 1: Peptidomimetics with different S substituents		
1	Cyclo(RLsKDK) s = D-serine	182 ± 23
2	Cyclo(RLSKDK) S = L-serine	240 ± 45
3	Cyclo(RLhS_βKDK) hS_β = β-homoserine	157 ± 32
4	Cyclo(RLA_βKDK) A_β = β-alanine	1645 ± 142
5	Cyclo(RLS*KDK) S* = (*S*)-3-carboxy-β-alanine	420 ± 53
Series 2: Peptidomimetics containing A_β		
6	Cyclo(R*LA_βKDK) R* = nitroarginine	2345 ± 123
7	Cyclo(R*LA_βKDK) R* = citrulline	890 ± 56
8	Cyclo(RL*A_βKDK) L* = *tert*-butylalanine	256 ± 16
9	Cyclo(RL*A_βKDK) L* = homoleucine	220 ± 28
10	Cyclo(RL*A_βKDK) L* = norleucine	378 ± 50
11	Cyclo(RL*A_βKDK) L* = norvaline	452 ± 63
12	Cyclo(RLA_βKDK*) K* = diaminopropionic acid	>5000
13	Cyclo(RLA_βKDK*) K* = diaminobutyric acid	>5000
14	Cyclo(RLA_βKDK*) K* = ornithine	>5000
15	Cyclo(RLA_βKDK*) K* = trimethyllysine	>10000
Series 3: Peptidomimetics containing hS_β		
16	Cyclo(R*LhS_βKDK) R* = nitroarginine	1245 ± 85
17	Cyclo(R*LhS_βKDK) R* = citrulline	192 ± 12
18	Cyclo(R*LhS_βKDK) R* = homoarginine	368 ± 32
19	Cyclo(RL*hS_βKDK) L* = homoleucine	142 ± 21

on the activity, while use of the neutral analogue citrulline (peptide **7**) led to an almost 2-fold increase in potency. These results indicate that arginine substitution by residues acting as hydrogen-bond acceptors favored inhibition of ADAM8 activity as opposed to charged and more sterically hindered ones. This trend was further exemplified in our third series (vide infra). Remarkably, substitution of leucine by homoleucine afforded peptide **9**, which showed much improved activity (~7-fold lower IC_{50}) than its parent peptide **4**. It was found from the biological data of peptides **9**–**11** that residues with more extended and flexible hydrophobic side-chains correlate with an increase in activity, thus suggesting the presence of a hydrophobic pocket at the receptor-binding site. Discrepancies in the results were observed when steric hindrance was introduced in the γ-position of the chain. While peptide **4** showed a ~4-fold drop in activity, peptide **8** containing a bulkier *tert*-butylalanine residue led to a ~1.5-fold improved IC_{50}, compare to **11**. All the analogues featuring modifications at ^{6}lysine (peptides **12**–**15**), showed a dramatic loss of

activity with IC_{50} values above 5000 nM. This highlights the importance of the KDK motif for binding to the integrin-binding loop of the ADAM8 disintegrin domain.

In our third series, we endeavoured to transpose both the arginine and leucine analogues which gave the best results within the β-alanine series to our new β-homoserine lead peptide **3**. We indeed hoped to observe a synergistic effect by introducing two favourable substitutions simultaneously within the parent peptide **1**. Interestingly, while peptides **17** and **19** showed increased activity compared to their β-alanine analogues **7** and **9**, with a ~4- and ~1.5-fold lower IC_{50}, respectively, it did not produce the similar 10-fold increase in potency observed in our first series when β-homoserine was employed in place of β-alanine. Despite peptide **19** being the most active analogue of our library, it only exhibited slightly higher inhibition than peptide **3**. In this series we also further investigated the effect of modifying the arginine residue. In β-homoserine-containing peptides **16** and **18**, the nitroarginine and the homoarginine were used in place of arginine, respectively. As previously observed introducing charged and bulky residues at this position had detrimental effects on the activity with a ~8- and ~2-fold increase in IC_{50} with respect to **3**. Although **17** showed improved inhibition activity compared to its β-alanine analogue **7**, it remained less active than **3**, thus suggesting that the prevailing interaction in the binding of **17** to its receptor occurs through the side-chain of the β-homoserine rather than that of the citrulline. The lack of a significant synergic effect observed in this series suggests that structural modifications which maximise the interaction of one residue, concurrently hinder the interaction of the other residue with the receptor.

In conclusion, we have identified two new strategies for the design of potent ligands of ADAM8 disintegrin domain. One consists of taking advantage of the receptor binding site involving the polar interaction observed with peptide **3** while the second focused on exploiting the hydrophobic pocket which is believed to be responsible for the improved binding of peptides **8**–**10**.

2.3. Conclusion

During this SAR study of the potent cyclo(RLsKDK) ADAM8 inhibitor, two prevalent modes of interactions between the ligand and the receptor were identified. Two peptidomimetics; cyclo(RLhS_{β}-KDK) **3** and cyclo(RhLA_{β}KDK) **9**; were found to present slightly increased activity compared to the lead peptide. Although the activity could not be significantly improved, these compounds could serve as potential new lead structures replacing cyclo (RLsKDK) for future SAR studies. Furthermore, it was established that Based on these promising results, additional work focusing on the design of a ligand capable of taking advantage of both the interaction sites described herein is on-going in our laboratory.

3. Experimental

3.1. General information

All reagents were purchased as reagent grade and used without further purification. HPLC solvents were purchased as HPLC grade and used without further purification. UV measurements were obtained using a Jenway 7315 spectrophotometer. Electrospray ionisation mass spectra (ESI-MS) were recorded on an Agilent Technologies 1120 Compact LC connected to a HP Series 1100 MSD spectrometer or a Bruker micrOTOF-Q II spectrometer. Samples were introduced using direct flow injection at 0.2 mL/min into an ESI source in positive mode, using 0.1% formic acid/H_2O and 0.1% formic acid/CH_3CN (1/1, v/v). Major and significant fragments were quoted in the form *x m/z* (mass to charge ratio). Analytical RP-HPLC was performed on a Dionex P680 system using a Waters XTerra® C18 column (5 μm, 4.6 × 150 mm) at a flow rate of 1 mL/min. A linear gradient of 0.1% TFA/H_2O (solvent A) and 0.1% TFA/CH_3CN (solvent B) was used with detection at 210 nm. Preparative RP-HPLC was performed on a Waters 600 System with a Waters 2487 dual wavelength absorbance detector using a Waters XTerra® Prep MS C18 column (10 μm, 19 × 300 mm) at a flow rate of 10 mL/min. Gradient systems were adjusted according to the elution profiles and peak profiles obtained from the analytical RP-HPLC chromatograms.

O-(7-azabenzotriazol-1-yl)-*N*,*N*,*N*′,*N*′-tetramethyluronium hexafluorophosphate (HATU), *O*-(benzotriazol-1-yl)-*N*,*N*,*N*′,*N*′-tetramethyluronium hexafluorophosphate (HBTU) and *O*-(6-Chlorobenzotriazol-1-yl)-*N*,*N*,*N*′,*N*′-tetramethyluronium hexafluorophosphate (HCTU) were purchased from Advanced ChemTech. *N*,*N*-dimethylformamide (DMF) and acetonitrile (CH_3CN) (synthesis grade) were purchased from Scharlau, and CH_2Cl_2 (synthesis grade) from ECP. Diisopropylethylamine ($^iPr_2NEt$), piperidine, triisopropylsilane ($^iPr_3SiH$), 4-(dimethylamino)pyridine (DMAP), *N*-methylmorpholine (NMM) were purchased from Sigma–Aldrich. *N*,*N*-Diisopropylcarbodiimide (DIC) was purchased from GL Biochem. 4-(4-hydroxymethyl-3-methoxyphenoxy) butyric acid (HMPB) was purchased from Merck. Trifluoroacetic acid (TFA) was purchased from Oakwood Chemicals. L-Amino acids were used unless otherwise stated. Fmoc-amino acids were purchased from GL Biochem, ChemImpex Inc., or PolyPeptide Laboratory. The catalyst $Pd(PPh_3)_4$[18] and aminomethyl PS resin[19] were synthesised according to published procedures.

3.2. General peptide synthesis procedures

Solid phase peptide synthesis (0.2 mmol scale) was performed on aminomethyl PS resin (1.0 mmol/g) based on the Fmoc based strategy. HMPB linker was attached to the resin using general method A, and coupling of the first amino acid residue to the HMPB-PS resin was performed according to general method B or C. The degree of attachment of the first amino acid residue to the resin was determined using UV spectrophotometry.[16] The desired peptide sequences were synthesised using general method D on Tribute™ peptide synthesiser, and peptide coupling of unnatural amino acids was performed manually according to general method E. The linear peptides were cleaved from the resin using general method F, and the crude products were cyclised using general method G. The side-chain protecting groups were removed from the cyclised peptides according to general method H, and the allyl protecting group was removed according to general method I. The crude peptides were purified according to general method J.

3.2.1. General method A: attachment of HMPB linker to aminomethyl PS resin

Aminomethyl PS resin (0.2 mmol) was swollen in CH_2Cl_2/DMF (1/1, v/v) for 20 min and the solvent was drained. HMPB (4 equiv) was dissolved in DMF/CH_2Cl_2 (3 mL, 5/95 v/v), and DIC (4 equiv) was added. The mixture was added to the resin, and the reaction was agitated for 2 h. The solution was drained, and the resin was washed with DMF (3×), CH_2Cl_2 (3×) and then air dried.

3.2.2. General method B: attachment of Fmoc-hS_{β}(O^tBu)-OH, Fmoc-β-Ala-OH, or Fmoc-Asp-OAll to HMPB-PS resin

To a solution of Fmoc protected amino acid (2 equiv) in DMF/CH_2Cl_2 (3 mL, 20/80 v/v) was added DIC (2 equiv), and the mixture was added to the HMPB-PS resin. DMAP (1 equiv) was added to the resin, and the reaction was stirred under MW irradiation (25 W, 50 °C) for 1 h. The solution was drained, and the resin was washed with DMF (3×) and CH_2Cl_2 (3×) and then air dried.

3.2.3. General method C: attachment of Fmoc-L-Ser(O^{t}Bu)-OH or Fmoc-D-Ser(O^{t}Bu)-OH to HMPB-PS resin

To a solution of Fmoc protected amino acid (4 equiv) in DMF/CH_2Cl_2 (3 mL, 20/80 v/v) was added DIC (4 equiv), and the mixture was added to the HMPB-PS resin. DMAP (0.1 equiv) was added to the resin, and the reaction was agitated for 2 h. The solution was drained, and the resin was washed with DMF (3×), CH_2Cl_2 (3×) and then air dried.

3.2.4. General method D: automated Fmoc SPPS

Couplings of Fmoc-Lys(Boc)-OH, Fmoc-Arg(Pbf)-OH, Fmoc-Asp(O^{t}Bu)-OH and Fmoc-Leu-OH (5 equiv) were carried out at room temperature in the presence of HCTU (4.6 equiv) and NMM (10 equiv) in DMF for 45 min. The Fmoc protecting group was removed using piperidine/DMF (3 mL, 20/80 v/v, 2 × 5 min).

3.2.5. General method E: manual coupling of unnatural amino acid

To a solution of Fmoc protected unnatural amino acid (2 equiv) in DMF (2 mL) was added HATU (1.85 equiv) and ^{i}Pr$_2$NEt (4 equiv), and the solution was added to the resin. After stirring under MW irradiation (25 W, 50 °C) for 1 h, the resin was drained, washed with DMF (3×), CH_2Cl_2 (3×) and then air dried. The Fmoc protecting group was removed using piperidine/DMF (3 mL, 20/80 v/v, 2 × 5 min).

3.2.6. General method F: cleavage of peptide from resin

The resin containing the desired linear peptide was agitated in TFA/CH_2Cl_2 (3 mL, 0.5/99.5 v/v) for 5 min, drained and the same procedure was repeated eight times. The combined filtrates (ca. 25 mL) were evaporated under a flow of N_2 gas, and the crude peptide was immediately dissolved in CH_3CN and lyophilised.

3.2.7. General method G: macrocyclisation

The linear peptide and HBTU (3 equiv) were dissolved in CH_2Cl_2/DMF (9/1, v/v), and the mixture was slowly added to a solution of ^{i}Pr$_2$NEt (5 equiv) in CH_2Cl_2/DMF (9/1, v/v) using a syringe pump at a rate of 0.5 mL/h to reach a final peptide concentration of 0.9 mg/mL. The solution was concentrated on a rotary evaporator, and the crude cyclic peptide was recovered by lyophilisation. For the synthesis of peptides **2** and **3**, HOBt (3 equiv) was added to the CH_2Cl_2/DMF solution containing the peptide and HBTU to prevent racemisation during cyclisation.

3.2.8. General method H: cleavage of side-chain protecting groups

The side-chain protecting groups on the crude cyclic peptide were removed by agitating in a solution of TFA/^{i}Pr$_3$SiH/H_2O (4 mL, 95/2.5/2.5 v/v) for 2 h. The crude peptide was precipitated from cold Et_2O, centrifuged, the supernatant decanted, and the same procedure was repeated. The resulting solid was dissolved in H_2O and lyophilised.

3.2.9. General method I: removal of allyl protecting group

The cyclic peptide was dissolved in argon degassed CH_2Cl_2 (1 mL). Pd(PPh$_3$)$_4$ (0.04 equiv) and $PhSiH_3$ (4 equiv) were added to the solution, and the reaction mixture was stirred under argon for 1 h, filtered, and the filtrate was concentrated under reduced pressure.

3.2.10. General method J: purification

The crude peptide was dissolved in H_2O and purified by preparative RP-HPLC on a XTerra® C18 column using a gradient of 0–60% B at 1% B/min with a flow rate of 10 mL/min. The purity of the peptide was determined by flow injection (ESI$^+$, 100 V) and analytical RP-HPLC (XTerra® C18 column, 5–95% B, 3% B/min, 1 mL/min).

3.3. Characterisation data

3.3.1. Cyclo(RLsKDK) s = D-serine (1)

Peptide **1** (13.0 mg, 9%) was obtained as a white solid in >99% purity according to analytical RP-HPLC. R_t = 6.4 min (XTerra® C18, 5–95% B, 3% B/min, 1.0 mL/min); *m/z* (ESI-MS): [M+H]$^+$ Calcd 728.4; Found 728.4.

3.3.2. Cyclo(RLSKDK) S = L-serine (2)

Peptide **2** (8.0 mg, 6%) was obtained as a white solid in >99% purity according to analytical RP-HPLC. R_t = 6.3 min (XTerra® C18, 5–95% B, 3% B/min, 1.0 mL/min); *m/z* (ESI-MS): [M+H]$^+$ Calcd 728.4; Found 728.4.

3.3.3. Cyclo(RLhS$_\beta$KDK) hS$_\beta$ = β-homoserine (3)

Peptide **3** (3 mg, 2%) was obtained as a white solid in >99% purity according to analytical RP-HPLC. R_t = 5.8 min (XTerra® C18, 5–95% B, 3% B/min, 1.0 mL/min); *m/z* (ESI-MS): [M+H]+ Calcd 742.5; Found 742.3.

3.3.4. Cyclo(RLA$_\beta$KDK) A$_\beta$ = β-alanine (4)

Peptide **4** (9.5 mg, 7%) was obtained as a white solid in >99% purity according to analytical RP-HPLC. R_t = 5.7 min (XTerra® C18, 5–95% B, 3% B/min, 1.0 mL/min); *m/z* (ESI-MS): [M+H]$^+$ Calcd 712.4; Found 712.3.

3.3.5. Cyclo(RLS*KDK) S* = (*S*)-3-carboxy-β-alanine (5)

Peptide **5** (0.3 mg, 0.1%) was obtained as a white solid in >99% purity according to analytical RP-HPLC. R_t = 7.1 min (XTerra® C18, 5–95% B, 3% B/min, 1.0 mL/min); *m/z* (ESI-MS): [M+H]$^+$ Calcd 756.4; Found 756.1.

3.3.6. Cyclo(R*LA$_\beta$KDK) R* = nitroarginine (6)

Peptide **6** (5 mg, 3%) was obtained as a white solid in >95% purity according to analytical RP-HPLC. R_t = 6.6 min (XTerra® C18, 5–95% B, 3% B/min, 1.0 mL/min); *m/z* (ESI-MS): [M+H]$^+$ Calcd 757.4; Found 757.4.

3.3.7. Cyclo(R*LA$_\beta$KDK) R* = citrulline (7)

Peptide **7** (19 mg, 13%) was obtained as a white solid in >99% purity according to analytical RP-HPLC. R_t = 5.4 min (XTerra® C18, 5–95% B, 3% B/min, 1.0 mL/min); *m/z* (ESI-MS): [M+H]$^+$ Calcd 713.4; Found 713.4.

3.3.8. Cyclo(RL*A$_\beta$KDK) L* = *tert*-butylalanine (8)

Peptide **8** (3.8 mg, 3%) was obtained as a white solid in >99% purity according to analytical RP-HPLC. R_t = 6.7 min (XTerra® C18, 5–95% B, 3% B/min, 1.0 mL/min); *m/z* (ESI-MS): [M+H]$^+$ Calcd 726.5; Found 726.5.

3.3.9. Cyclo(RL*A$_\beta$KDK) L* = homoleucine (9)

Peptide **9** (4.5 mg, 3%) was obtained as a white solid in >99% purity according to analytical RP-HPLC. R_t = 6.9 min (XTerra® C18, 5–95% B, 3% B/min, 1.0 mL/min); *m/z* (ESI-MS): [M+H]$^+$ Calcd 726.5; Found 726.4.

3.3.10. Cyclo(RL*A$_\beta$KDK) L* = norleucine (10)

Peptide **10** (1.7 mg, 1%) was obtained as a white solid in >99% purity according to analytical RP-HPLC. R_t = 10.4 min (XTerra® C18, 5–95% B, 3% B/min, 1.0 mL/min); *m/z* (ESI-MS): [M+H]$^+$ Calcd 711.4; Found 712.3.

3.3.11. Cyclo(RL*A$_\beta$KDK) L* = norvaline (11)

Peptide **11** (1.7 mg, 1%) was obtained as a white solid in >95% purity according to analytical RP-HPLC. R_t = 6.3 min (XTerra® C18,

5–95% B, 3% B/min, 1.0 mL/min); *m*/*z* (ESI-MS): $[M+H]^+$ Calcd 697.4; Found 698.2.

3.3.12. Cyclo(RLA$_\beta$KDK*) K* = diaminopropionic acid (12)

Peptide **12** (2.5 mg, 2%) was obtained as a white solid in >99% purity according to analytical RP-HPLC. R_t = 9.3 min (XTerra® C18, 5–95% B, 3% B/min, 1.0 mL/min); *m*/*z* (ESI-MS): $[M+H]^+$ Calcd 669.4; Found 670.4.

3.3.13. Cyclo(RLA$_\beta$KDK*) K* = diaminobutyric acid (13)

Peptide **13** (6.4 mg, 5%) was obtained as a white solid in >99% purity according to analytical RP-HPLC. R_t = 6.0 min (XTerra® C18, 5–95% B, 3% B/min, 1.0 mL/min); *m*/*z* (ESI-MS): $[M+H]^+$ Calcd 683.4; Found 684.5.

3.3.14. Cyclo(RLA$_\beta$KDK*) K* = ornithine (14)

Peptide **14** (1.4 mg, 1%) was obtained as a white solid in >99% purity according to analytical RP-HPLC. R_t = 5.8 min (XTerra® C18, 5–95% B, 3% B/min, 1.0 mL/min); *m*/*z* (ESI-MS): $[M+H]^+$ Calcd 697.4; Found 698.4.

3.3.15. Cyclo(RLA$_\beta$KDK*) K* = trimethyllysine (15)

Peptide **15** (2.0 mg, 1%) was obtained as a white solid in >99% purity according to analytical RP-HPLC. R_t = 6.0 min (XTerra® C18, 5–95% B, 3% B/min, 1.0 mL/min); *m*/*z* (ESI-MS): $[M+H]^+$ Calcd 754.5; Found 754.4.

3.3.16. Cyclo(R*LhS$_\beta$KDK) R* = nitroarginine (16)

Peptide **16** (6.4 mg, 4%) was obtained as a white solid in >99% purity according to analytical RP-HPLC. R_t = 6.8 min (XTerra® C18, 5–95% B, 3% B/min, 1.0 mL/min); *m*/*z* (ESI-MS): $[M+H]^+$ Calcd 786.4; Found 787.4.

3.3.17. Cyclo(R*LhS$_\beta$KDK) R* = citrulline (17)

Peptide **17** (0.9 mg, 0.6%) was obtained as a white solid in >99% purity according to analytical RP-HPLC. R_t = 7.8 min (XTerra® C18, 5–95% B, 3% B/min, 1.0 mL/min); *m*/*z* (ESI-MS): $[M+H]^+$ Calcd 742.4; Found 743.5.

3.3.18. Cyclo(R*LhS$_\beta$KDK) R* = homoarginine (18)

Peptide **18** (0.8 mg, 0.5%) was obtained as a white solid in >95% purity according to analytical RP-HPLC. R_t = 6.4 min (XTerra® C18, 5–95% B, 3% B/min, 1.0 mL/min); *m*/*z* (ESI-MS): $[M+H]^+$ Calcd 756.5; Found 756.1.

3.3.19. Cyclo(R*LhS$_\beta$KDK) R* = homoleucine (19)

Peptide **19** (2.3 mg, 2%) was obtained as a white solid in >95% purity according to analytical RP-HPLC. R_t = 7.2 min (XTerra® C18, 5–95% B, 3% B/min, 1.0 mL/min); *m*/*z* (ESI-MS): $[M+H]^+$ Calcd 755.5; Found 756.1.

3.4. Inhibition of ADAM8-mediated CD23 release from cells by cyclic peptides

The ability of cyclic peptides to inhibit ADAM8-mediated shedding of CD23 from COS7 cells was measured using an ELISA as described.[13] COS7 cells co-transfected with CD23 and ADAM8 cDNA were seeded out in 12-well plates at a density of 2×10^5 cells/well with or without peptides (range between 10 nM and 10 μM) for 6 h. After 6 h, the amounts of CD23 released in the supernatants were determined using a commercial CD23 ELISA (R&D Systems, UK). The standards were prepared as eight serial 1:2 dilutions ranging from 400 to 12.5 units/mL. Blank and sample duplicates (each 100 μL) were also applied, after that 50 μL of diluted biotinylated anti-CD23 monoclonal antibody (1/100) was added. After application of all required solutions the plate was incubated for 2 h at room temperature. The multiwell plate was then emptied and washed 4 times with washing buffer to remove the unbound biotin conjugates and re-incubated with 100 μL per well of diluted streptavidin–HRP (1/100) for l h at room temperature. After additional washing of the plate, TMB substrate solution (100 μL/well) was added for 10–20 min until colour development. Absorbance in each individual well was determined using an ELISA plate reader (BMG Labtech, Offenburg, Germany) at 405 nm. The amount of soluble CD23 released from COS7 cells when using the cyclic peptides is reduced to an extent that reflects the contribution of ADAM8 to the overall cleavage of CD23 in these cells.[5]

Acknowledgment

The authors thank Cancer Research UK for financial support.

Supplementary data

Supplementary data (structures and LC–MS profiles of synthetic peptides) associated with this article can be found, in the online version, at http://dx.doi.org/10.1016/j.bmc.2016.06.042.

References and notes

1. Edwards, D. R.; Handsley, M. M.; Pennington, C. J. *Mol. Aspects Med.* **2008**, *29*, 258.
2. Kelly, K.; Hutchinson, G.; Nebenius-Oosthizen, D.; Smith, A. J. H.; Bartsch, J. W.; Horiuchi, K.; Rittger, A.; Manova, K.; Docherty, A. J. P.; Blopel, C. P. *Dev. Dyn.* **2005**, *232*, 221.
3. Schlomann, U.; Rathke-Hartlieb, S.; Yamamoto, S.; Jockusch, H.; Bartsch, J. W. *J. Neurosci.* **2000**, *20*, 7964.
4. King, N. E.; Zimmermann, N.; Pope, S. M.; Fulkerson, P. C.; Nikolaidis, N. M.; Mishra, A.; Witte, D. P.; Rothenberg, M. E. *Am. J. Respir. Cell Mol. Biol.* **2004**, *31*, 257.
5. Fourie, A. M.; Coles, F.; Moreno, V.; Karlsson, L. *J. Biol. Chem.* **2003**, *278*, 30469.
6. (a) Ishikawa, N.; Daigo, Y.; Yasui, W.; Inai, K.; Nishimura, H.; Tsuchiya, E.; Kohno, N.; Nakamura, Y. *Clin. Cancer Res.* **2004**, *10*, 8363; (b) Roemer, A.; Schwettmann, L.; Jung, M.; Stephan, C.; Roigas, J. A. N.; Kristiansen, G.; Loening, S. A.; Lichtinghagen, R.; Jung, K. *J. Urol.* **2004**, *172*, 2162.
7. Wildeboer, D.; Naus, S.; Sang, Q.-X. A.; Bartsch, J. W.; Pagenstecher, A. *J. Neuropathol. Exp. Neurol.* **2006**, *65*, 516.
8. Moss, M. L.; Bartsch, J. W. *Biochemistry* **2004**, *43*, 7227.
9. Schlomann, U.; Wildeboer, D.; Webster, A.; Antropova, O.; Zeuschner, D.; Knight, C. D.; Docherty, A. J.; Lambert, M.; Skelton, L.; Jockusch, H.; Bartsch, J. W. *J. Biol. Chem.* **2002**, *277*, 48210.
10. Reiss, K.; Saftig, P. *Semin. Cell Dev. Biol.* **2009**, *20*, 126.
11. (a) Rothenberg, M. L.; Nelson, M. R.; Hande, K. R. *Stem Cells* **1999**, *17*, 237; (b) Sparano, J. A.; Bernardo, P.; Stephenson, P.; Gradishar, W. J.; Ingle, J. N.; Zucker, S.; Davidson, N. E. *J. Clin. Oncol.* **2004**, *22*, 4683.
12. Bartsch, J.; Koller, G. *Protease Inhibition*. WO Patent 2,009,047,523, 2009.
13. Schlomann, U.; Koller, G.; Conrad, C.; Ferdous, T.; Golfi, P.; Garcia, A. M.; Höfling, S.; Parsons, M.; Costa, P.; Soper, R.; Bossard, M.; Hagemann, T.; Roshani, R.; Sewald, N.; Ketchem, R. R.; Moss, M. L.; Rasmussen, F. H.; Miller, M. A.; Lauffenburger, D. A.; Tuveson, D. A.; Nimsky, C.; Bartsch, J. W. *Nat. Commun.* **2015**, *6*, 6175. http://dx.doi.org/10.1038/ncomms7175 (in press).
14. Weisshoff, H.; Prasang, C.; Henklein, P.; Frommel, C.; Zschunke, A.; Mugge, C. *Eur. J. Biochem.* **1999**, *259*, 776.
15. Egner, B. J.; Cardno, M.; Bradley, M. *J. Chem. Soc., Chem. Commun.* **1995**, *21*, 2163.
16. Chan, W. C.; White, P. D. In *Fmoc Solid Phase Peptide Synthesis*; Oxford University Press, 2000; pp 62–63.
17. Kaur, H.; Heapy, A. M.; Brimble, M. A. *Synlett* **2012**, *23*, 2284.
18. Coulson, D. R.; Satek, L. C.; Grim, S. O. In *Inorg. Synth*; Cotton, F. A., Ed.; John Wiley & Sons, 2007; pp 121–124.
19. Harris, P. W. R.; Brimble, M. A. *Synthesis* **2009**, *20*, 3460.